Science of the Total Environment 461–462 (2013) 10–18

Contents lists available at SciVerse ScienceDirect

Science of the Total Environment

journal homepage: www.elsevier.com/locate/scitotenv

Dynamics of CO_2 fluxes and environmental responses in the rain-fed winter wheat ecosystem of the Loess Plateau, China

Wen Wang, Yuncheng Liao *, Xiaoxia Wen, Qiang Guo

College of Agronomy, Northwest A&F University, Yangling, Shaanxi 712100, China

HIGHLIGHTS

- The winter wheat ecosystem acted as a strong carbon sink.
- Environmental responses of CO2 fluxes varied with different ranges of factors.
- Response of CO2 fluxes to environmental factors varied with soil water conditions.
- Strong fluctuations of CO2 fluxes usually appeared after effective rainfall events.
- Strong fluctuations of CO2 fluxes also occurred within 5days after sowing.

ARTICLE INFO

Article history:
Received 8 May 2012
Received in revised form 1 April 2013
Accepted 23 April 2013
Available online 24 May 2013

Editor: Christian EW Steinberg

Keywords:
Net ecosystem CO_2 exchange
Ecosystem respiration
Eddy covariance technique
Environmental response mechanism
Environmental factor

ABSTRACT

Chinese Loess Plateau plays an important role in carbon balance of terrestrial ecosystems. Continuous measurement of CO_2 fluxes in cropland ecosystem is of great significance to accurately evaluate the carbon sequestration potential and to better explain the carbon cycle process in this region. By using the eddy covariance system we conducted a long-term (from Sep 2009 to Jun 2010) CO_2 fluxes measurement in the rain-fed winter wheat field of the Chinese Loess Plateau and elaborated the responses of CO_2 fluxes to environmental factors. The results show that the winter wheat ecosystem has distinct seasonal dynamics of CO_2 fluxes. The total net ecosystem CO_2 exchange (NEE) of -218.9 ± 11.5 gC m^{-2} in the growing season, however, after considering the harvested grain, the agro-ecosystem turned into a weak carbon sink (-36.2 gC m^{-2}). On the other hand, the responses of CO_2 fluxes to environmental factors depended on different growth stages of winter wheat and different ranges of environmental variables, suggesting that the variations in CO_2 exchange were sensitive to the changes in controlling factors. Particularly, we found the pulse response of ecosystem respiration (R_{eco}) to a large rainfall event, and the strong fluctuations of CO_2 fluxes usually appeared after effective rainfall events (daily precipitation > 5 mm) during middle growing season. Such phenomenon also occurred in the case of the drastic changes in air temperature and within 5 days after field management (e.g. tillage and plough).

1. Introduction

In recent years, sustainable development across the globe has been severely restricted by the negative impacts of global climate change. Considering the fact that carbon cycling in terrestrial ecosystems plays an important role in global carbon balance and that carbon exchange at regional scale exerts direct influence on regional climate change, monitoring and understanding carbon cycling processes have become a major focus of regional sustainable development as well as global climate change. Cropland ecosystem is a critical component of the terrestrial ecosystems and its carbon pool is of vital importance to maintain the global carbon balance. Thus long-term measurement of CO_2 exchange and evaluation of carbon budget may provide theoretical guidance for laying down measures to reduce carbon emissions and improve carbon sequestration.

Since the 1980s, based on eddy covariance (EC) technique, many researchers have endeavored to measure and analyze the potential of carbon sequestration in terrestrial ecosystems. Although previous studies mainly focused on forest and grassland ecosystems (Hernandez-Ramirez et al., 2011), the study on the characteristics of the CO_2 exchange in cropland ecosystem is gradually increasing in academic field. Scientists have carried out detailed study on inter- and intra-annual variations of CO_2 fluxes (Aubinet et al., 2009; Moors et al., 2010; Glenn et al., 2010). Some of them have conducted research on the methods of data quality assessment and data processing

* Corresponding author at: Tel.: +86 29 87082990; fax: +86 29 87082845.
E-mail address: yunchengliao@nwsuaf.edu.cn (Y. Liao).

0048-9697
http://dx.doi.org/10.1016/j.scitotenv.2013.04.068

(Soegaard et al., 2003; Anthoni et al., 2004; Saito et al., 2005). Others have reported the responses of CO_2 fluxes to environmental factors. For instance, the relationships between physiological characteristics of crops and CO_2 fluxes at different crop growth stages (Moureaux et al., 2008; Hoyaux et al., 2008), the variations in CO_2 fluxes under different meteorological conditions (Béziat et al., 2009; Dufranne et al., 2011), the relationship between daytime net ecosystem CO_2 exchange (NEE) and photosynthetically active radiation (PAR) under different water conditions (Pingintha et al., 2010), the effects of temperatures on ecosystem respiration (R_{eco}) in different periods (Moureaux et al., 2006; Hernandez-Ramirez et al., 2011) and different crop sites (Suyker et al., 2004), and the impact of agricultural management practices on carbon balance (Ceschia et al., 2010; Eugster et al., 2010; Glenn et al., 2010). Winter wheat with exclusive worldwide distribution, at present, there are a small number of Chinese scholars who have conducted research on estimating the carbon budget (Li et al., 2006; Li et al., 2007; Lei and Yang, 2010) and analyzing the environmental responses of CO_2 fluxes in winter wheat ecosystem (Li et al., 2006; Yan et al., 2009), whereas most of them are mainly located in Huang-Huai-Hai plain, China.

The Loess Plateau covers an area of 64×10^4 km^2 in Northwest China, including 14.5×10^4 km^2 of arable land. More than 70% of crop plant in rain-fed land, which is much more susceptible to climate change impacts. Thus, measurement of CO_2 exchange in the rain-fed field is of great significance to better understand the relationship between the carbon cycling and climatic change in the region. Based on the eddy covariance (EC) system, we performed continuous observation (from Sep 2009 to Jun 2010) in the rain-fed winter wheat field of the Chinese Loess Plateau. The main objectives of this study were to: (1) elaborate the dynamics of CO_2 fluxes and estimate the carbon budget in growing season; (2) analyze the response mechanisms of CO_2 fluxes to environmental factors.

2. Materials and methods

2.1. Site description

The experimental field (latitude 35°14′ N, longitude 107°41′ E, 1220 m above mean sea level) is situated at the Changwu agro-ecological experiment site, which is located in the central-southern part of Chinese Loess Plateau, Shaanxi Province. This region belongs to warm continental monsoon climate zone. Mean annual global solar radiation and mean annual temperature at the Changwu site are 484 kJ cm^{-2} and 9.1 °C, respectively (mean values computed over 20 years from 1986 to 2005). Mean annual accumulated temperature of ≥0 °C is 3688 °C, and ≥10 °C is 3029 °C, with mean annual sunshine duration of 2226.5 h and a frost-free period of 171 days. Mean annual precipitation is 584.1 mm and mainly in July to September, which accounts for more than 55% of the total. Multiple cropping index is 116%. Groundwater depth is 50–80 m. The soil type of the field is dark loessial soil. In September 2009, the soil organic matter and soil organic carbon content in the first 0.3 m were 11.58 and 6.74 g kg^{-1}, respectively. This region is a typical rain-fed agricultural area with single cropping system and without irrigation. The soil nutrient and topographic characteristics of the experimental field are quite representative of the similar areas in the Chinese Loess Plateau.

The field has an approximate area of 100 m × 100 m and has flat terrain with eddy covariance (EC) system installed in the middle. This field has been cultivated for more than 30 years and within the range of the field all crops grown were winter wheat, which forms homogeneous underlying surface in order to satisfy the requirement of the fetch in the prevailing wind directions. The tested winter wheat cultivar was Changwu 134 with sowing rate of 150 kg ha^{-1} and row spacing of 0.2 m. The winter wheat growth stages based on the Zadoks scale (Zadoks et al., 1974) are listed in Table 1. The conventional tillage by a rotary harrow to a depth of 25 cm was performed during sowing. 120 kg ha^{-1} mineral N, 90 kg ha^{-1} phosphorus and 62 kg ha^{-1} potassium had been applied to the arable layer as base fertilizer in September 2009. Note that no farmyard manure and no irrigation were applied during the growing season.

Table 1
Winter wheat growth stages in Changwu site during the 2009–2010 growing season.

Growth stage	Date
Sowing	26-Sep-2009
Seedling stage	03-Oct-2009
Tillering stage	22-Oct-2009
Winter dormancy stage	11-Nov-2009
Stem elongation stage	11-Mar-2010
Booting stage	22-Apr-2010
Heading stage	15-May-2010
Grain filling stage	04-Jun-2010
Ripening stage	20-Jun-2010
Harvesting	25-Jun-2010

2.2. Measurements

CO_2 flux (F_c), latent heat flux (LE) and sensible heat flux (H_s) were measured by the eddy covariance (EC) system positioned 2 m above the soil surface. Three-dimensional wind velocity and virtual temperature were measured with a 3D sonic anemometer (Gill Instruments Ltd., UK). The densities of CO_2 and water vapor were measured with a LI-7500 open-path infrared CO_2/H_2O gas analyzer (LI-COR Inc., USA). The data from the sonic anemometer and the CO_2/H_2O gas analyzer were recorded at 10 Hz on a CR5000 data logger (Campbell Scientific Inc., USA).

Other relevant instruments were as follows: photosynthetically active radiation radiometer (LI-COR Inc., USA), 3-Cup Anemometer (Vaisala Inc., Finland), temperature-humidity sensors (Vaisala Inc., Finland), soil temperature–moisture sensor (Campbell Scientific Inc., USA) at depths of 0.02, 0.1, 0.2, 0.4, and 0.8 m, two soil heat flux plates (Hukseflux, Delft, Netherlands) at depth of 0.05 m and a tipping bucket rain gage (Campbell Scientific Inc., USA). All the above mentioned instruments used CR10X data logger (Campbell Scientific Inc., USA) to collect and store data.

A LI-3000 portable leaf area meter (LI-COR Inc., USA) was utilized to measure the leaf area index (LAI) bi-weekly from seedling stage to winter dormancy stage and weekly from stem elongation stage to ripening stage. LAI was expressed as one-half the total leaf area per unit ground area (m^2 m^{-2}). At harvest, grain yield was measured by gathering grains from three zones of 2 m × 50 m.

2.3. Data analysis and processing

The original data from the EC measurements were processed off-line using the software MATLAB 7.5 (Math works Inc., USA). The half-hourly CO_2 fluxes were computed by the eddy covariance method as the mean covariance between fluctuations in vertical wind velocity (w', m s^{-1}) and the CO_2 density (ρ_c', mg m^{-3}). Thereafter, the CO_2 fluxes were corrected by a 3D coordinate rotation in order to align the sensor of 3D sonic anemometer in the mean streamline direction (Wilczak et al., 2001), and then they were corrected for fluctuations of air and water vapor density according to the Webb–Pearman–Leuning (WPL) algorithm (Webb et al., 1980).

Besides, some studies have demonstrated that even for short crops (e.g. winter wheat, rice) the CO_2 storage term should be considered when calculate CO_2 fluxes (Soegaard et al., 2003; Saito et al., 2005). To measure the change of CO_2 storage below the EC sensor, a single height (at the height of EC measurement, 2 m) method according to Moureaux et al. (2008) was applied. Thus, the NEE value was

calculated as the sum of the half-hourly EC measured CO_2 flux and the rate of change in CO_2 storage below the EC sensor:

$$NEE = F_c + F_s \quad (1)$$

where F_c is CO_2 flux ($mgCO_2\ m^{-2}\ s^{-1}$) after the 3D Rotation correction and the WPL correction. F_s is CO_2 storage. We comply with the convention that CO_2 away from the soil is considered as positive and those towards the soil as negative.

Half-hourly EC data were rejected according to these criteria: (1) incomplete half-hourly datasets, (2) the fluxes under stable nighttime conditions (nighttime was defined as PAR < 5 μmol $m^{-2}\ s^{-1}$ and solar elevation angles < 0°) when friction velocity (u*) was less than 0.15 m s^{-1}, and (3) the EC data were submitted to a stationary test and integral turbulence characteristic test. The software used in the study generated flags (1 to 9) according to the data quality control proposed by Foken et al. (2004). The higher the class of the flag indicated the higher the level of the data quality in the EC data. In this study, the data of classes 1 to 3 were used for analyzing the relationships between CO_2 fluxes and environmental factors, and the data of class 9 was rejected.

To further evaluate the data quality, a flux footprint analysis was performed using the flux source area model (FSAM). The method for experimental field evaluation has been elaborated by Schmid (2002). The result showed that more than 90% of the flux contribution came from the study area during daytime, however, approximately 75% of flux contribution from the study area during nighttime because of atmospheric stability conditions. Overall, it suggested that the measured fluxes are totally representative of the study area, even under the stable conditions. Meanwhile, the energy balance closure was tested using a linear regression between the half-hourly EC fluxes ($LE + H_s$) and the available energy ($R_n - G$). The relationship we observed was: $(LE + H_s) = 0.91(R_n - G) + 9.39$, with determination coefficient (R^2) of 0.92, indicating that the EC measurements underestimate $LE + H_s$ by 9%, which is consistent with previous studies (Wilson et al., 2002).

Missing data due to sensor malfunction, power failure and data rejection accounted for 17.2% of total original EC data. The Missing data were gap-filled using:

1) For small gaps within 2 h, the missing data were linearly interpolated.
2) For larger data gaps over 2 h and the corresponding meteorological data remained complete, the daytime gaps were filled by using the relationship between NEE and incident PAR based on 10-day periods (Falge et al., 2001):

$$F_{NEE,day} = -\frac{\alpha \cdot Q_P \times P_{max}}{\alpha \cdot Q_P + P_{max}} + R_d \quad (2)$$

where $F_{NEE,\ day}$ is the net ecosystem CO_2 exchange during daytime ($mgCO_2\ m^{-2}\ s^{-1}$), α is the ecosystem quantum yield

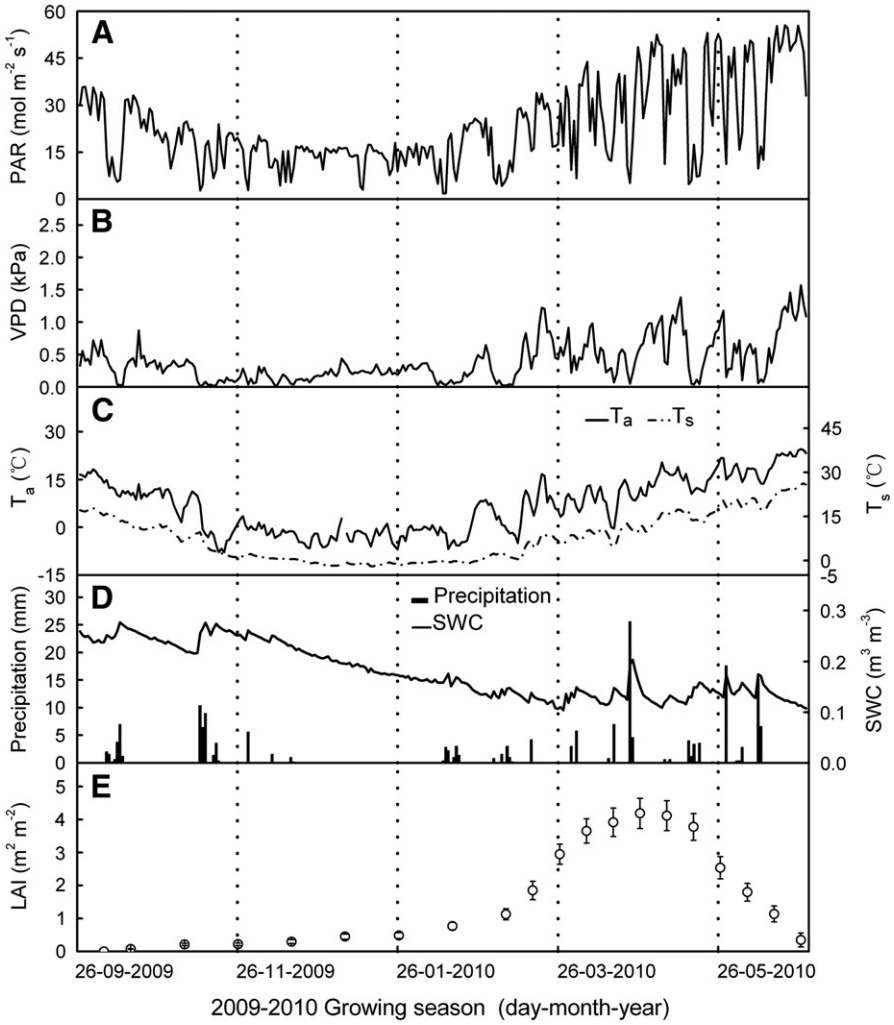

Fig. 1. Variations of environmental factors in Changwu site during the 2009–2010 growing season. A. Daily total photosynthetically active radiation (PAR); B. Daily mean vapor pressure deficit (VPD); C. Daily mean air temperature (T_a) and daily mean soil temperature (T_s) at 0.02 m depth; D. Daily accumulated precipitation and daily mean soil water content (SWC) at 0–0.2 m depth; E. Variation of leaf area index (LAI). Error bars denote the mean ± SE ($p < 0.05$).

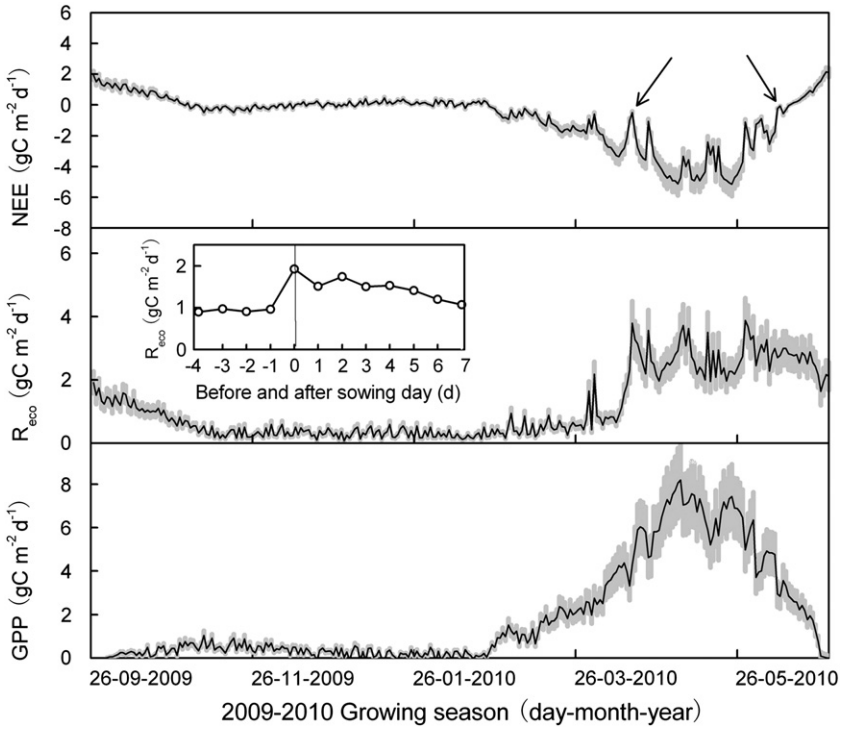

Fig. 2. Dynamics of net ecosystem CO_2 exchange (NEE), ecosystem respiration (R_{eco}) and gross primary productivity (GPP) during the 2009–2010 growing season. Shaded area represents the uncertainty. The inset figure depicts the dynamics of the daily R_{eco} before and after sowing day.

($mgCO_2$ μmol^{-1} photons), P_{max} is the net photosynthetic rate at light saturation ($mgCO_2$ m^{-2} s^{-1}), Q_P is the incident PAR (μmol m^{-2} s^{-1}), R_d is the ecosystem respiration rate during daytime ($mgCO_2$ m^{-2} s^{-1}).

Nighttime data gaps were filled by using the bi-weekly empirical relationships between nighttime ecosystem respiration and soil temperature under windy conditions ($u^* > 0.15$ m s^{-1}) (Lloyd and Taylor, 1994):

$$F_{R,night} = F_{R,10} e^{E_0[(1/(283.15-T_0))-(1/(T_s-T_0))]} \quad (3)$$

where $F_{R,\ night}$ is the ecosystem respiration flux during nighttime ($mgCO_2$ m^{-2} s^{-1}), $F_{R,10}$ is the respiration rate ($mgCO_2$ m^{-2} s^{-1}) at 10 °C (283.15 K), E_0 is the temperature sensitivity of respiration (K), T_0 is the temperature at which ecosystem respiration is zero (K), T_s is the soil temperature at 0.02 m depth (K).

3) In the case of missing meteorological data, the method of mean diurnal variation (MDV) (Falge et al., 2001) was applied using data windows of 10 days.

Table 2
Accumulated CO_2 fluxes (NEE, R_{eco} and GPP) with uncertainties during each growth stage.

Growing season	NEE (gC m^{-2})	R_{eco} (gC m^{-2})	GPP (gC m^{-2})	Sink/source
Sowing to seedling stage	22.8 ± 1.2	24.5 ± 2.7	2.0 ± 3.0	Source
Tillering stage	6.6 ± 0.4	15.1 ± 1.4	8.4 ± 1.5	Source
Winter dormancy stage	−7.8 ± 0.5	35.2 ± 2.8	43.0 ± 2.8	Sink
Stem elongation stage	−65.3 ± 4.5	39.1 ± 3.3	104.4 ± 5.6	Sink
Booting stage	−104.2 ± 7.6	73.1 ± 6.1	177.3 ± 9.7	Sink
Heading stage	−74.7 ± 5.3	47.2 ± 4.2	121.9 ± 6.8	Sink
Grain filling stage to harvest	3.8 ± 0.2	59.4 ± 5.2	55.4 ± 5.2	Source
Growing season total	−218.9 ± 11.5	293.7 ± 15.3	512.4 ± 19.1	Sink

Daytime R_{eco} was extrapolated from Eq. (3). Ecosystem respiration (R_{eco}) was the sum of daytime R_{eco} and nighttime R_{eco}. Gross primary productivity (GPP) was calculated as the difference between R_{eco} and NEE. The NEE uncertainty caused by the random error was assessed according to the methodology of Richardson and Hollinger (2007) using the Monte Carlo simulation. The R_{eco} uncertainty was calculated as the quadratic sum of the partitioning uncertainty and the intrinsic dispersion uncertainty. The GPP uncertainty was estimated as the quadratic sum of the NEE and the R_{eco} uncertainties (Dufranne et al., 2011). Regression analyses were used to examine the relationships between CO_2 fluxes and environmental factors. Statistical analyses were performed using SPSS 17.0 (SPSS Inc., USA).

3. Results

3.1. Variations of environmental factors

The environmental factors showed distinct seasonal trends during the 2009–2010 growing season. (Fig. 1) We observed the similar seasonal trends of PAR and vapor pressure deficit (VPD) during the growing season (Fig. 1A, B). Average temperature during the 2009–2010 growing season was 6.7 °C, which was a little higher than the long-term average (6.5 °C, average value measured between 1986 and 2005). The variation of the soil temperature (T_s) at 0.02 m depth was consistent with the air temperature (T_a) during the growing season (Fig. 1C). Precipitation in the growing season (185.7 mm) was a little larger than the average (172.3 mm), and distribution of rainfall was uneven in the growing season (Fig. 1D). Range of daily average soil water content (SWC, 0–0.2 m depth) was 0.30–0.10 m^3 m^{-3}, which experienced a steady-state decrease through the growing season (Fig. 1D). Besides, leaf area was very varied in different growth stages. Leaf area index (LAI) reached a peak value of 4.19 ± 0.38 m^2 m^{-2} in late April 2010 (Fig. 1E). In general, the meteorological conditions and soil moisture status were fairly representative of the regional long-term averages.

Table 3
Accumulated NEE for winter wheat growing season after considering carbon in the grain (C_{gr}) at different crop sites.

Crop site	Crop type	Growing season	Grain yield (g m^{-2})	Carbon in grain C_{gr} (gC m^{-2})	Seasonal NEE (gC m^{-2})	NEE + C_{gr} (gC m^{-2})	Reference
Changwu, China	Winter wheat	2009–2010	472.1	182.7	−218.9	−36.2	This study
Thuringia, Germany	Winter wheat	2001	739	286	−185 to −245	41–101	Anthoni et al. (2004)
Yucheng, China	Winter wheat	2002–2003	526.0	203.6	−77.6	126.0	Li et al. (2006)
		2003–2004	543.0	210.1	−152.2	57.9	
Weishan, China	Winter wheat	2005–2006	645	250	−326	−76	Lei and Yang (2010)
		2006–2007	675	261	−394	−133	
		2007–2008	637	247	−303	−56	
		2008–2009	656	295	−395	−100	

3.2. Dynamics of CO_2 fluxes

The dynamics of the CO_2 fluxes showed distinct seasonal trends during the winter wheat growing season (Fig. 2). Form seedling stage to tillering stage, the net CO_2 uptake rate remained lower than the ecosystem respiration, thus the ecosystem behaved as small carbon source (Table 2). During winter dormancy stage, daily NEE varied around zero, and the ecosystem acted as weak carbon sink (Table 2). In stem elongation stage, the NEE curve dropped significantly, and the accumulated NEE during the stage was -65.3 ± 4.5 gC m^{-2} day^{-1}, the ecosystem acted as moderate carbon sink (Table 2). During booting stage, the ecosystem became strong carbon sink (Fig. 2). From grain filling stage to ripening stage, NEE curve rose sharply, and the ecosystem was characterized by a weak carbon source (Table 2). Finally, total NEE, R_{eco}, and GPP for the growing season were -218.9 ± 11.5, 293.7 ± 15.3, and 512.4 ± 19.1 gC m^{-2} (Table 2), respectively, suggesting that the ecosystem acted as a strong carbon sink and had relatively high photosynthetic productivity during the growing season.

On a regional scale, crop grains are harvested and eventually consumed, thus all the carbon in harvested grain is released back into the atmosphere. We hypothesized that all of the wheat straws were returned to the field, and carbon in the grain (C_{gr}, gC m^{-2}) was calculated as:

$$C_{gr} = \left(1 - W_{gr}\right) f_C Y \quad (4)$$

where W_{gr} is the grain water content (14% for winter wheat), f_C is the fraction of carbon in the grain (0.45 for wheat), and Y is the yield (gC m^{-2}). Considering that the carbon released by grains, the ecosystem switched from a strong carbon sink to a weak carbon sink (-36.2 gC m^{-2}) (Table 3). This suggests that the carbon sequestration of the winter wheat ecosystem is more than the amount of carbon consumed in the form of grain after considering the carbon in the grain.

3.3. Responses of CO_2 fluxes to environmental factors

3.3.1. Response of CO_2 fluxes to LAI

In winter wheat growth season, a significant relationship was found between seasonal variation of NEE and LAI (Fig. 3A). In the case of given incident PAR (1300–1500 μmol m^{-2} s^{-1}), the determination coefficient (R^2) with the 95% confidence level, was 0.8214 ($p = 0.0228$) at early growing season (seedling stage to tillering stage), 0.8856 ($p = 0.0124$) at middle growing season (stem elongation stage to heading stage), and 0.7052 ($p = 0.0413$) at late growing season (grain filling stage to ripening stage), respectively (Fig. 3A), suggesting that LAI is one of the driving factors for the seasonal variation of NEE. The correlation analysis ($p = 0.0342$) showed that seasonal dynamics of net photosynthetic rate at light saturation (P_{max}) was closely related to the seasonal change of LAI (Fig. 3B). Note that in the late growing season, the correlation was lower and a sharp decrease of P_{max}, mainly because of a reduction in photosynthesis during leaf senescence and an increase in soil respiration under relatively high temperature.

3.3.2. Responses of CO_2 fluxes to PAR and VPD

A significantly negative correlation was observed between NEE and PAR at different growth stages (Fig. 4A). The R^2 with the 95% confidence level, was respectively 0.9542 ($p < 0.0001$) at stem elongation stage, 0.9716 ($p < 0.0001$) at booting stage, and 0.9677 ($p < 0.0001$) at heading stage (Fig. 4A), indicating that PAR is a predominant factor contributing to the dynamics of NEE during daytime. To analyze the correlation between NEE and PAR under different weather conditions, clear sky conditions (the ratio of diffuse PAR to total PAR (d/t) < 0.5) and cloudy sky conditions (d/t > 0.5) at booting stage and heading stage were selected. The result showed that the R^2 in the cloudy sky conditions ($R^2 = 0.9706$, 95% confidence level, $p < 0.0001$) was higher than that in the clear sky conditions ($R^2 = 0.9045$, 95% confidence level, $p < 0.0001$) (Fig. 4B), because of a distinct reduction of net CO_2 uptake rate at around noon caused by midday stomata closure in clear weather

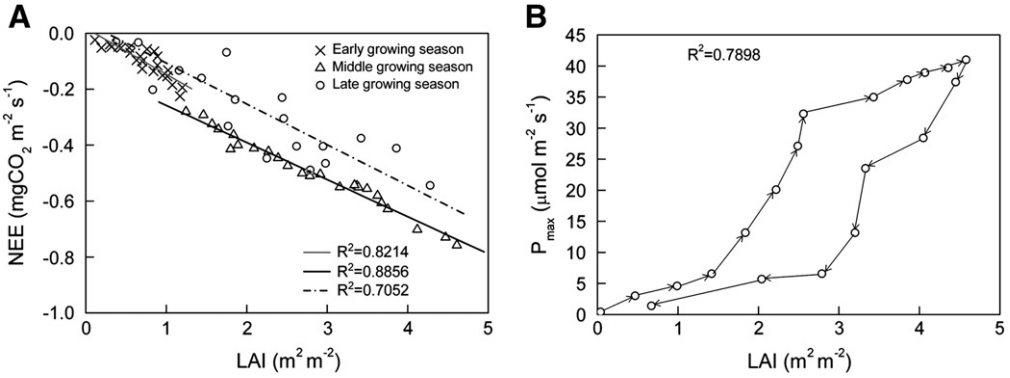

Fig. 3. A. Relationship between NEE at given PAR (between 1300 and 1500 μmol m^{-2} s^{-1}) and LAI at early growing season (n = 25), middle growing season (n = 26) and late growing season (n = 23); B. Relationship between net photosynthetic rate at light saturation (P_{max}) and LAI in the growing season (n = 20). The arrows denote the process of time.

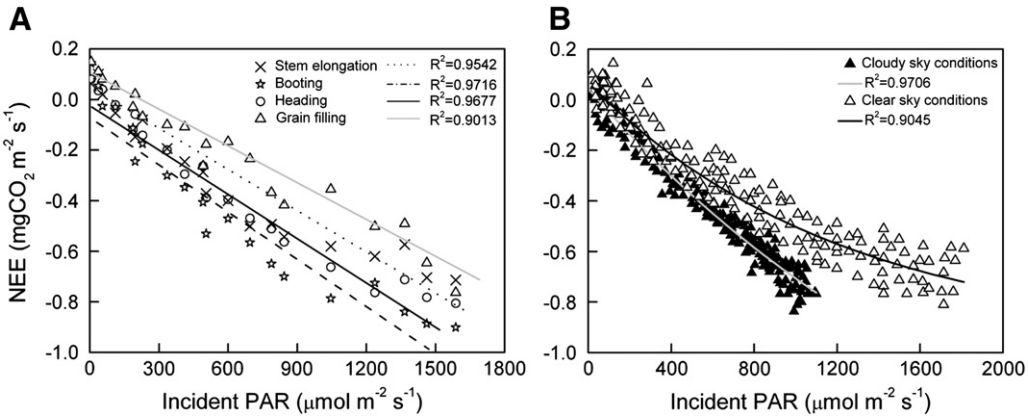

Fig. 4. A. Response of the daytime NEE to incident PAR at stem elongation stage (n = 20), booting stage (n = 22), heading stage (n = 21) and grain filling stage (n = 20); B. Response of the NEE to incident PAR under the clear sky conditions (ratio of diffuse PAR to total PAR (d/t) < 0.5, n = 235) and the cloudy sky conditions (d/t > 0.5, n = 231) during booting stage and heading stage.

with higher PAR (Jarvis and Morrison, 1981). Thus, PAR is probably the most important driving factor for fluctuations of NEE during cloudy sky conditions (Béziat et al., 2009).

Besides, no significant correlation (80% confidence level, $p = 0.0878$) existed between daily NEE and VPD in the middle growing season (Fig. 5A). Initially, net CO_2 uptake rate tended to increase with a rise in VPD and, then, decrease obviously with the increase of VPD as VPD above 1.4 kPa (Fig. 5A). We found the different values of R^2 between NEE and PAR for the different ranges of VPD from booting stage to heading stage. The correlation in the VPD range from 0 to 1.4 kPa ($R^2 = 0.8691$, 95% confidence level, $p = 0.0002$) was higher than that in the VPD range from 1.4 to 2.5 kPa ($R^2 = 0.7816$, 95% confidence level, $p = 0.0013$) (Fig. 5B). That could be explained by the reduction of net CO_2 uptake rate due to a decrease of stomatal conductance as VPD over 1.4 kPa.

3.3.3. Response of CO_2 fluxes to temperature

The correlation between nighttime R_{eco} and soil temperature (T_s) at 0.02 m depth varied in the different growing stages (Fig. 6). The R^2 was 0.8417 (95% confidence level, $p = 0.0086$) at stem elongation stage and 0.8310 (95% confidence level, $p = 0.0133$) at booting stage and heading stage, respectively, which were much higher than that at late growing season ($R^2 = 0.6127$, 95% confidence level, $p = 0.0254$) (Fig. 6), suggesting that the variations in R_{eco} were sensitive to the changes in T_s during the middle growing season, when temperature was a predominant limiting factor for growth of plants and activity of microbial community.

3.3.4. Responses of CO_2 fluxes to SWC

Different relationships were found between daytime NEE and PAR under different SWC conditions (Fig. 7). When soil moisture was sufficient ($0.15 \le SWC < 0.25\ m^3\ m^{-3}$), the daytime net CO_2 uptake rate increased with PAR (Fig. 7A). For lower SWC ($SWC < 0.15\ m^3\ m^{-3}$), the net CO_2 uptake rate increased with PAR before noon and then decreased substantially as PAR above 1100 μmol $m^{-2}\ s^{-1}$ (Fig. 7A). Furthermore, when SWC was higher than $0.25\ m^3\ m^{-3}$, the response of NEE to PAR was smaller than that under conditions of sufficient soil moisture. Similar relationships were also observed between nighttime R_{eco} and T_s at 0.02 m depth under different SWC conditions (Fig. 7B). The correlation under water sufficient conditions was higher than the correlation under water deficit conditions and the correlation under water excess conditions.

3.3.5. Pulse response of CO_2 fluxes to rainfall events

Fig. 8 shows that the CO_2 fluxes were sensitive to the effective rainfall events (daily precipitation > 5 mm) during the middle growing season. We observed the drastic changes in maximum daily half-hourly R_{eco} and NEE following a large rainfall event (on 20-Apr-2010 with daily precipitation of 25.6 mm). The daily maximum half-hourly R_{eco} reached the peaks within 1–2 days after the effective rainfall events, which were about 0.5- to 6.5-fold larger than that in the pre-rain days (Fig. 8A). The maximum half-hourly NEE (absolute value) occurred 3–6 days after the effective rainfall events, which were about 0.5- to 1.5-fold larger than that in the pre-rain days (Fig. 8B). By using the EC system, the rain-induced pulses of R_{eco} have

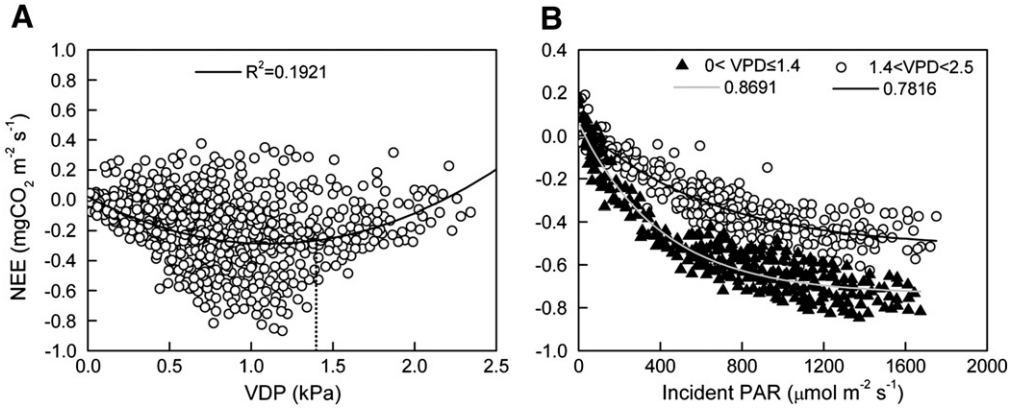

Fig. 5. A. Response of NEE to VPD during the growing season (n = 1108); B. Relationship between NEE and incident PAR at $0 < VPD \le 1.4$ (n = 280) and $1.4 < VPD < 2.5$ (n = 282) during booting stage and heading stage.

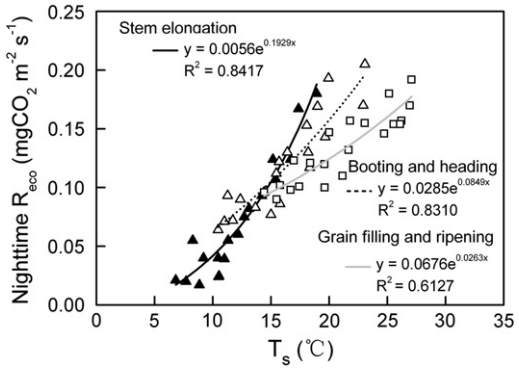

Fig. 6. Relationship between nighttime ecosystem respiration (R_{eco}) and soil temperature (T_s) at 0.02 m depth at stem elongation stage (n = 21, full triangle), booting and heading stages (n = 20, empty triangle), and grain filling and ripening stages (n = 21, empty square).

also been reported in other arid and semi-arid ecosystems (Huxman et al., 2004; Lee et al., 2004; Xu et al., 2004).

4. Discussion

4.1. Complex responses of CO_2 fluxes to SWC

Complex response mechanisms were found between CO_2 fluxes and environmental factors under different SWC (Fig. 7). For lower SWC, net CO_2 uptake rate decreased substantially as PAR above 1100 μmol m^{-2} s^{-1} (Fig. 7A), which was caused by midday stomata closure as solar radiation, air temperature, and VPD were all high under water deficit stress (Jarvis and Morrison, 1981). A similar phenomenon has been demonstrated by Pingintha et al. (2010) in a Georgia peanut ecosystem. Meanwhile, under higher SWC, the response of NEE to PAR was smaller than that under sufficient soil moisture conditions (Fig. 7A). This is probably because the suppression of photosynthesis is associated with poor soil aeration or oxygen deficiency under the high SWC conditions (Gliński and Stepniewski, 1985). Furthermore, the effect of SWC on ecosystem respiration became more significant under water stress, when activities of microbial community were restricted (Davidson et al., 1998). Overall, different soil moisture conditions could complicate the response mechanism of CO_2 fluxes to other environmental factors. Thus, combining with the chamber method and biometric measurements to further explain the environmental response of CO_2 fluxes to different water conditions will be important.

4.2. Strong fluctuations of the NEE

Strong fluctuations of the NEE were found during the middle stages, when plants were in active growth. There are several reasons for this: Firstly, following the large rainfall event (on 20-Apr-2010 with daily precipitation of 25.6 mm), considerable CO_2 released into the atmosphere, which can be several orders of magnitude greater than the pre-rain days (Fig. 8), because the large rainfall event significantly triggered microbial respiration, and the percolating rainwater physically displaced soil air rich in CO_2 and squeezed out CO_2 into atmosphere (Orchard and Cook, 1983; Borken et al., 2003). The instant increase in CO_2 release is probably because the water became deficit for shallow layer following soil gradually dried out and then inhibited microbial activity (Huxman et al., 2004). Noting that during the large rainfall event the net CO_2 uptake rate was small (Fig. 8), because the photosynthesis of winter wheat was consumed by its own respiration. However, after the rainfall event, the net CO_2 uptake rate eventually increased, lagging a few days behind the response of R_{eco} (Fig. 7), mainly because the sufficient soil water in the root zone could stimulate root and leaf growth and improve photosynthesis.

Secondly, during the active growth stages, the drastic changes in air temperature usually led to the obvious variations in NEE curve. For example, from 13-Apr-2010 to 14-Apr-2010, the average air temperature dropped sharply to around 0 °C (Fig. 1C). The cold weather led to a steep rise in NEE curve and then a rapid decline as the air temperature increased (Fig. 2). In the late stage of grain filling, notice the sudden transitions from negative NEE values to positive NEE values (Fig. 2), probably because the photosynthetic capacity fell sharply, whereas the soil respiration varied with the particular meteorological conditions, for example, soil respiration increased significantly in the case of high temperature along with rainfall events during this period.

In addition, the higher R_{eco} was observed within 5 days after sowing (Fig. 2), mainly because the field management (e.g. tillage and plough) has been shown to stimulate soil CO_2 emission by increasing aeration, changing soil temperature and moisture conditions, disrupting soil aggregates and thus favoring soil microbial respiration. Within 5 days after sowing, we observed that the daily R_{eco} was 0.5–1.0 gC m^{-2} day^{-1} higher than that before field management (Fig. 2). Ceschia et al. (2010) and Eugster et al. (2010) have reported that after field management, the high CO_2 emissions from agro-ecosystems continued for the first few days and up to 3–6 weeks.

4.3. A comparison of different study results

Considering the carbon released by grains, the winter wheat ecosystem acted as a weak carbon sink (−36.2 gC m^{-2}) during the growing

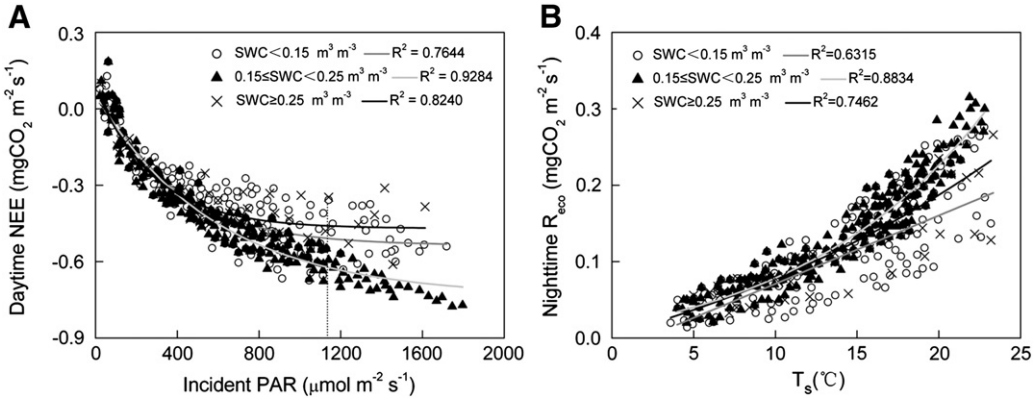

Fig. 7. A. Response of daytime NEE to incident PAR under SWC < 0.15 m^3 m^{-3} (n = 205), 0.15 ≤ SWC < 0.25 m^3 m^{-3} (n = 201) and SWC ≥ 0.25 m^3 m^{-3} (n = 40), p < 0.01; B. Response of nighttime R_{eco} to soil temperature (T_s) at 0.02 m depth (p < 0.05) under SWC < 0.15 m^3 m^{-3} (n = 207), 0.15 ≤ SWC < 0.25 m^3 m^{-3} (n = 202) and SWC ≥ 0.25 m^3 m^{-3} (n = 41), p < 0.01.

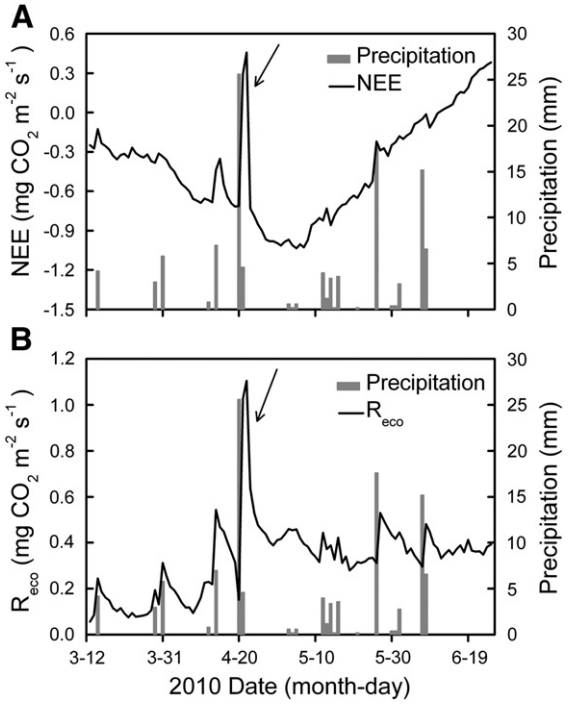

Fig. 8. Dynamics of A daily maximum half-hourly NEE and B daily maximum half-hourly R_{eco} in the middle and late growing seasons.

season. The result is consistent with the report of Lei and Yang (2010) (Table 3). However, some studies reported that winter wheat ecosystem behaved as carbon sources (41–126 gC m^{-2}) after considering the carbon in grain (Anthoni et al., 2004; Li et al., 2006) (Table 3). These differences can be explained, in part, by the geographical environment, climate condition, soil type, cropping system and some other uncontrollable factors vary in different crop sites. On the other hand, it is probably because of different field management practices (e.g. non-irrigation vs. irrigation; conventional tillage vs. minimum tillage or no-tillage) as well as data processing methods and some other controllable factors (e.g. the starting and ending time for estimating carbon budget of the growing season).

5. Conclusions

The present study demonstrates that the rain-fed winter wheat ecosystem of the Chinese Loess Plateau has the distinct dynamics of CO_2 fluxes and the total NEE for the growing season was -218.9 ± 11.5 gC m^{-2}, suggesting that the ecosystem acted as a strong carbon sink, whereas after considering the harvested grain, the ecosystem turned into a weak carbon sink. The responses of CO_2 fluxes to the controlling factors depended on the different growth stages of winter wheat and different ranges of environmental variables, indicating that the variations in CO_2 fluxes were sensitive to the changes in some environmental factors, such as LAI, PAR, T_s and SWC. Particularly, the pulse response of R_{eco} to the large rainfall event was observed, and the strong fluctuations of CO_2 fluxes generally occurred after the effective rainfall events (daily precipitation > 5 mm) during the middle growing season. Such phenomenon also takes place in the case of the drastic changes in T_a and within 5 days after sowing.

Acknowledgments

This study was funded by the National Science Foundation of China (Grant No. 31171506 and No. 31071375) and the Programme of Introducing Talents of Discipline to Universities (No. B12007). We thank Prof. Shengli Guo and Prof. Wenzhao Liu, Institute of Soil and Water Conservation, Chinese Academy of Sciences, for their valuable assistance during the study.

References

Anthoni PM, Freibauer A, Kolle O, Schulze E-D. Winter wheat carbon exchange in Thuringia, Germany. Agric Meteorol 2004;121:55–67.
Aubinet M, Moureaux C, Bodson B, Dufranne D, Heinesch B, Suleau M, et al. Carbon sequestration by a crop over a 4-year sugar beet/winter wheat/seed potato/winter wheat rotation cycle. Agric Meteorol 2009;149:407–18.
Béziat P, Ceschia E, Dedieu G. Carbon balance of a three crop succession over two cropland sites in South West France. Agric Meteorol 2009;149:1628–45.
Borken W, Davidson EA, Savage K, Gaudinskib J, Trumborec SE. Drying and wetting effects on carbon dioxide release from organic horizons. Soil Sci Soc Am J 2003;67:1888–96.
Ceschia E, Béziata P, Dejoux JF, Aubinet M, Bernhofer C, Bodson B, et al. Management effects on net ecosystem carbon and GHG budgets at European crop sites. Agric Ecosyst Environ 2010;139:363–83.
Davidson EA, Belk E, Boone RD. Soil water content and temperature as independent or confounded factors controlling soil respiration in a temperate mixed hardwood forest. Glob Chang Biol 1998;4:217–27.
Dufranne D, Moureaux C, Vancutsem F, Bodson B, Aubinet M. Comparison of carbon fluxes, growth and productivity of a winter wheat crop in three contrasting growing seasons. Agric Ecosyst Environ 2011;141:133–42.
Eugster W, Moffat AM, Ceschia E, Aubinet M, Ammann C, Osborne B, et al. Management effects on European cropland respiration. Agric Ecosyst Environ 2010;139:346–62.
Falge E, Baldocchi D, Olson R, Anthoni P, Aubinet M, Bernhofer C, et al. Gap filling strategies for defensible annual sums of net ecosystem exchange. Agric Meteorol 2001;107:43–69.
Foken T, Goeckede M, Mauder M, Mahrt L, Amiro BD, Munger JW. Postfield data quality control. In: Lee X, Massman WJ, Law B, editors. Handbook of micrometeorology: a guide for surface flux measurement and analysis. Holand: Kluwer Academic Publishers; 2004.
Glenn AJ, Amiro BD, Tenuta M, Stewart SE, Wagner-Riddle C. Carbon dioxide exchange in a northern Prairie cropping system over three years. Agric Meteorol 2010;150:908–18.
Gliński J, Stepniewski W. Soil aeration and its role for plants. Florida: CRC Press; 1985.
Hernandez-Ramirez G, Hatfield JL, Parkin TB, Sauer TJ, Prueger JH. Carbon dioxide fluxes in corn–soybean rotation in the midwestern U.S.: inter- and intra-annual variations, and biophysical controls. Agric Meteorol 2011;151:1831–42.
Hoyaux J, Moureaux C, Tourneur D, Bodson B, Aubinet M. Extrapolating gross primary productivity from leaf to canopy scale in a winter wheat crop. Agric Meteorol 2008;148:668–79.
Huxman TE, Snyder KA, Tissue D, Leffler AJ, Ogle K, Pockman WT, et al. Precipitation pulses and carbon fluxes in semiarid and arid ecosystems. Oecologia 2004;141:254–68.
Jarvis PG, Morrison JIL. The control of transpiration and photosynthesis by the stomata. In: Jarvis PG, Mansfield TA, editors. Stomatal physiology. Cambridge: Cambridge University Press; 1981.
Lee XH, Wu HJ, Sigler J, Oishi C, Siccama T. Rapid and transient response of soil respiration to rain. Glob Chang Biol 2004;10:1017–26.
Lei HM, Yang DW. Seasonal and interannual variations in carbon dioxide exchange over a cropland in the North China Plain. Glob Chang Biol 2010;16:2944–57.
Li J, Yu Q, Sun X, Tong X, Ren C, Wang J, et al. Carbon dioxide exchange and the mechanism of environmental control in a farmland ecosystem in North China Plain. Sci China Ser D 2006;49(Supplement II):226–40.
Li SJ, Liu WZ, Takahashi A, Hiyama T, Fukushima Y, Li Z, et al. The seasonal variation of CO_2 flux in a wheat field of the Loess Plateau. Acta Ecol Sin 2007;27:1987–92. [in Chinese].
Lloyd J, Taylor J. On the temperature dependence of soil respiration. Funct Ecol 1994;8:315–23.
Moors EJ, Jacobs C, Jans W, Supit I, Kutsch WL, Bernhofer C, et al. Variability in carbon exchange of European croplands. Agric Ecosyst Environ 2010;139:325–35.
Moureaux C, Debacq A, Bodson B, Heinesch B, Aubinet M. Annual net ecosystem carbon exchange by a sugar beet crop. Agric Meteorol 2006;139:25–39.
Moureaux C, Debacq A, Hoyaux J, Suleau M, Tourneur D, Bodson B, et al. Carbon balance assessment of a Belgian winter wheat crop (*Triticum aestivum* L.). Glob Chang Biol 2008;14(6):1353–66.
Orchard VA, Cook FJ. Relationship between soil respiration and soil moisture. Soil Biol Biochem 1983;22:153–60.
Pingintha N, Leclerc MY, Beasley JP, Durden D, Zhang G, Senthong C, et al. Hysteresis response of daytime net ecosystem exchange during drought. Biogeosciences 2010;7:1159–70.
Richardson AD, Hollinger DY. A method to estimate the additional uncertainty in gap-filled NEE resulting from long gaps in the CO_2 flux record. Agric Meteorol 2007;147:199–208.
Saito M, Miyata A, Nagai H, Yamada T. Seasonal variation of carbon dioxide exchange in rice paddy field in Japan. Agric Meteorol 2005;135:93-109.
Schmid HP. Footprint modelling for vegetation atmosphere exchange studies: a review and perspective. Agric Meteorol 2002;113:159–83.
Soegaard H, Jensen NO, Boegh E, Hasager CB, Schelde K, Thomsen A. Carbon dioxide exchange over agricultural landscape using eddy correlation and footprint modeling. Agric Meteorol 2003;114:153–73.
Suyker AE, Verma SB, Burba GG, Arkebauer TJ, Walters DT, Hubbard KG. Growing season carbon dioxide exchange in irrigated and rainfed maize. Agric Meteorol 2004;124:1-13.

Webb EK, Pearman GI, Leuning R. Correction of flux measurement for density effects due to heat and water vapor transfer. Q J R Meteorol Soc 1980;106:85-100.
Wilczak JM, Oncley SP, Stage SA. Sonic anemometer tilt correction algorithms. Bound-Lay Meteorol 2001;99:127–50.
Wilson K, Goldstein A, Falge E, Aubinet M, Baldocchi D, Berbigier P, et al. Energy balance closure at FLUXNET sites. Agric Meteorol 2002;113:223–43.
Xu LK, Baldocchi DD, Tang JW. How soil moisture, rain pulses, and growth alter the response of ecosystem respiration to temperature. Glob Biogeochem Cycles 2004;18:1-10.
Yan HM, Fu YL, Xiao XM, Huang HQ, He HL, Ediger L. Modeling gross primary productivity for winter wheat-maize double cropping system using MODIS time series and CO_2 eddy flux tower data. Agric Ecosyst Environ 2009;129:391–400.
Zadoks JC, Chang TT, Konzak CF. A decimal code for the growth stages of cereals. Weed Res 1974;14:415–21.